Experimental control of vortex breakdown by density effects

Mohd-Zulhilmi Paiz Ismadi,[1,2,a)] Patrice Meunier,[1,3] Andreas Fouras,[1] and Kerry Hourigan[1,2]
[1]*Division of Biological Engineering, Monash University, Melbourne, Victoria 3800, Australia*
[2]*Department of Mechanical and Aerospace Engineering, Monash University, Melbourne, Victoria 3800, Australia*
[3]*Institut de Recherche sur les Phénomenes Hors Equilibre, Aix-Marseille University, 13384 Marseille, France*

(Received 21 November 2010; accepted 31 January 2011; published online 11 March 2011)

The vortex breakdown inside a cylinder with a rotating top lid is controlled experimentally by injecting at the bottom a fluid with a small density difference. The density difference is obtained by mixing a heavy dye or alcohol with water in order to create a jet denser or lighter than water. The injection of a heavy fluid creates a buoyancy force downward, which counteracts the meridional recirculation in the cylinder and thus enhances the formation of a vortex breakdown bubble. The stability diagram shows that even a very small density difference of 0.02% is able to decrease by a factor of 2 the critical Reynolds number of appearance of the breakdown. On the other hand, the injection of a lighter fluid does not destroy the vortex breakdown. However, for large enough density differences (larger than 0.03%), the lighter fluid is able to pierce through the bubble and leads to a new structure of the vortex breakdown. Finally, a parallel is drawn between a light jet and a vortex ring generated at the bottom of the cylinder: strong vortex rings are able to pierce through the bubble, whereas weak vortex rings are simply advected around the bubble. © *2011 American Institute of Physics*. [doi:10.1063/1.3560386]

I. INTRODUCTION

Vortex breakdown usually refers to a recirculating bubble that appears on a swirling jet past a stagnation point. The goal of this paper is to analyze the sensitivity of this flow to a small injection of dense or light fluid in the core of the vertical swirling jet.

Vortex breakdown is a surprising and practically important phenomenon which can be observed in many different swirling flows. It appears as a rapid expansion of a thin vortex into a much broader vortex with an axisymmetric or spiralling recirculating pattern.[1] The phenomenon is of interest for various disciplines due to its occurrence in geophysical as well as in industrial swirling flows. Vortex breakdown was first observed over the delta wings of aircraft[2–4] where it creates a sudden drop in the lift and an increase in the drag, possibly leading to a loss of aircraft control.[5] By contrast, it can be advantageous in geophysical applications since it largely decreases the swirl of the vortex and thus limits the destructive power of tornadoes.[6,7] It is also beneficial in combustion devices since the presence of vortex breakdown can be used as a flame holder.[8] Additionally, vortex breakdown is of interest in bioengineering applications for the growth of cells inside bioreactors. New bioreactors made of cylinders with a rotating top disk have been proposed recently.[9,10] They create a smooth and efficient mixing inside the cylinder which brings more oxygen to the cells and thus accelerate their growth. On one hand, the presence of vortex breakdown might prevent the mixing of oxygen in the whole cylinder and thus decrease the efficiency of these bioreactors. On the other hand, the vortex breakdown bubble could be used to localize the cells in a region far from the boundaries in order to prevent their adhesion to the wall and to reduce the destructive shear that they experience at the boundaries.

Vortex breakdown is also of great interest on a fundamental level. Despite a large amount of research in the past five decades, the destabilizing mechanism is not well understood. Early experiments have focused on flows in a tube, where the swirl is created by adjustable vanes located upstream of the tube.[11–13] They have shown that the bubble can be axisymmetric, helical, or contain a double helix, depending on the swirl parameter and the Reynolds number, with a strong hysteresis between these three regimes.

Theoretically, the early explanation of vortex breakdown as a helical instability[14] has been dismissed due to the presence of axisymmetric bubbles. Since these axisymmetric bubbles are observed for flows with no axisymmetric instability, another mechanism has to be found. Benjamin[15] explained vortex breakdown as a transition from a supercritical flow (without waves propagating upstream) to a subcritical flow (with waves propagating upstream) analogous to a hydraulic jump. This theory validates the criterion proposed by Squire[16] on the swirl parameter and has been recently extended to pipes with finite sizes by Wang and Rusak.[17]

Vortex breakdown has later been observed in a more simple configuration consisting of a closed cylinder with a rotating bottom.[18,19] This confined swirling flow has the great advantage of having very weak disturbances and well-defined boundary conditions. However, this flow does not have a constant swirl parameter in the volume of the cylinder and Benjamin's theoretical criterion is thus harder to apply.

a)Electronic mail: zac.ismadi@monash.edu.

The stability properties of this flow have been measured accurately by Escudier:[20] vortex breakdown appears in a finite band of the Reynolds number if the height to radius ratio H/R of the cylinder is larger than 1.5. Spohn *et al.*[21] later showed that this behavior is quantitatively but not qualitatively modified by the presence of a free surface.

Many numerical studies[22–24] have focused on the vortex breakdown inside a cylinder with a rotating bottom due to its confinement and its simple boundary conditions. They confirmed the stability diagram established by Escudier[20] and highlighted the role of negative azimuthal vorticity.[25] Furthermore, simulations confirmed that breakdown bubbles can become unsteady and asymmetric[26] as had been found experimentally.

Despite its interest for applications, there have been very few attempts to control vortex breakdown. Numerically, vortex breakdown was controlled by the corotation of the end walls[27,28] or by using the theory of optimal control in a closed loop system.[29] It has also been controlled numerically by applying a small temperature difference[30] between the bottom and the top disk, which leads to small density differences sufficient to stabilize or destabilize the vortex breakdown by gravitational and centrifugal convection. More recently, vortex breakdown was controlled by the rotation of a small rod,[31] a small lid,[32] or a small disk[33] opposite to the driving disk. Finally, it was shown that the use of a conical lid strongly influences the stability of vortex breakdown.[34]

Experimentally, there are few publications of control of vortex breakdown. One idea tested was the rotating of a small rod at the center of the cylinder.[35] This intrusive technique was replaced by a nonintrusive one where a small disk is rotated at the other end of the cylinder.[36] The authors reached a variation of 15% of the critical Reynolds number when the small disk is rotated twice faster than the driving disk. Other examples of control are axial pulsing[37] and lid tilting.[38]

In this paper, we apply experimentally the idea of Herrada and Shtern[30] to control the vortex breakdown by density effects. We use a slightly different setup since the density is introduced by injecting a fluid with a different density than the fluid inside the cylinder at the center of the motionless disk. We will show that this jet has a strong effect on vortex breakdown even for small injection rates and small density differences. After describing the experimental setup in Sec. II, we recover the literature results for a neutrally buoyant jet in Sec. III. We then describe the effect of a dense and a light jet in Secs. IV and V, respectively. Finally, we draw a parallel between the injection of a lighter jet and the generation of a vortex ring impacting the vortex breakdown in Sec. VI. Conclusions follow in Sec. VII.

II. EXPERIMENTAL SETUP AND METHODS

We study the flow inside a circular cylinder with a rotating top disk. Figure 1 shows the experimental setup, consisting of a cylindrical Plexiglas container with internal radius R=32.5 mm, filled with water. This inner cylinder is placed inside an octagonal housing, which is also filled with water and which has flat exterior faces to prevent the refraction

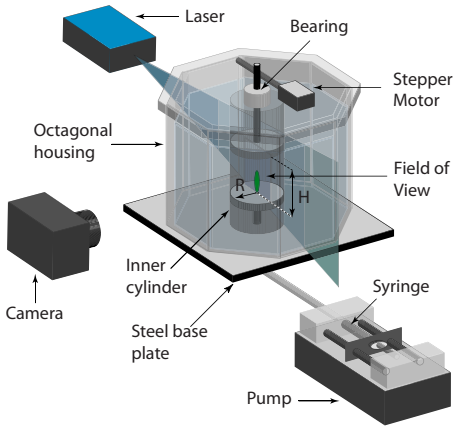

FIG. 1. (Color online) Diagram of the experimental setup used for the vortex breakdown inside the inner cylinder with a rotating top disk and with injection of dye at the bottom.

deformation of the images during the acquisition process. The whole setup is mounted on a steel base plate which is secured to a precision optical table to eliminate mechanical vibrations.

The flow under study is located inside the inner cylinder between two disks separated by a height H. For all the experimental cases, the aspect ratio H/R is maintained constant at 1.98, measured to an accuracy of 0.02%. In most previous experimental studies,[20,39] the bottom disk is rotated in order to drive the flow. Here, the bottom disk is fixed instead and the top disk is rotated at an angular velocity Ω varying from 0.6 to 3.6 rad/s. This top disk is driven by a stepper motor (Sanyo Denki America, Inc., USA) run through a motion controller (National Instruments Australia, North Ryde, NSW, Australia), enabling 5.12×10^4 steps per revolution. The velocity of the motor is further reduced by a factor 30 through the use of a worm wheel gear, which allows a smooth rotation of the disk at all speeds.

The flow is visualized by injecting some dye mixture at the center of the bottom disk through a 0.5 mm hole. The disturbance created by the hole itself is negligible. The hole is connected by a small plastic tube to a 1 ml syringe, filled with dye mixture, and driven by a syringe pump (Harvard Apparatus, Massachusetts, USA) at a volumic rate Q varying between 0.001 and 0.2 ml/min. In most experiments, the injection rate is equal to 0.02 ml/min, which gives a velocity of the jet equal to 1.7 mm/s, i.e., much smaller than the velocity of the disk periphery varying from 20 to 120 mm/s. Moreover, the characteristic time of variation of the mean density in the cylinder ($\tau=\pi R^2H/Q$) is on the order of 10^4 min, which is much larger than the duration of the experiments, which is on the order of a few minutes. This means that the mean density inside the cylinder can be assumed to be constant.

The fluorescein dye is illuminated by a blue laser (CVI Melles Griot, New Mexico, USA) so that it fluoresces very brightly with a green color. As illustrated in Fig. 1, the laser is expanded into a vertical sheet which is carefully placed at the center of the inner cylinder to visualize the flow pattern in a longitudinal section. A digital camera, Nikon D2X fitted

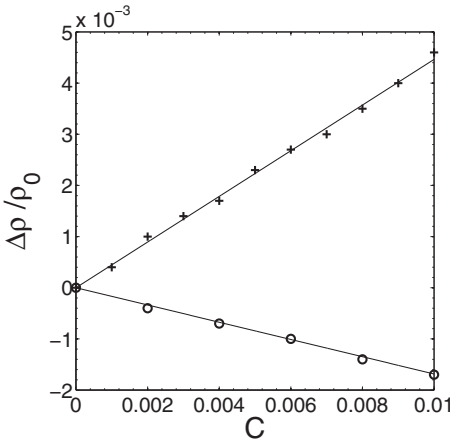

FIG. 2. Relative density difference $\Delta\rho/\rho_0=(\rho-\rho_0)/\rho_0$ of a fluorescein mixture (+) and of an alcoholic mixture (○) compared to water as a function of the mass concentration. Solid lines correspond to linear fit shown in Eqs. (1) and (2).

with Nikkor 17–55 mm f2.8G lens (Nikon Corporations, Japan) is used to capture the images of the dye during the experiments.

The temperature of the water is measured with an accuracy of 0.5 °C, which gives an accuracy of 1% on the viscosity. The average temperature of the room is fairly constant (less than 1°/day) such that thermal gradients can be ignored due to the small working fluid volume inside the inner cylinder (213.5 ml) and good forced mixing effect in the working area.

To study the effect of the density of the dye on the vortex breakdown, we have changed the density by varying the concentration of the dye (for heavier dye) and by adding alcohol (for lighter dye) in the mixture. A specific amount (usually 0.2 g) of fluorescein powder ($C_{20}H_{12}O_5$) is weighed using a precision balance (CP153, Sartorius Mechatronics, Australia) (with an accuracy of 0.001 g) and diluted in 100 ml of water, then diluted again to reach the desired mass concentration C, i.e., the weight of fluorescein divided by the weight of water. A similar protocol is conducted for the alcohol mixture except that a specific volume of 99.99% pure liquid ethanol is added into 100 ml of water and then diluted to the desired mass concentration. Although both mixtures are kept in closed flasks, a new mixture of ethanol is used for each experiment to eliminate the possibility of density change as a consequence of evaporation.

The density ρ of the dye and alcohol mixtures can be measured for large enough concentrations C using a density meter (Densito 30PX, Mettler Toledo, USA) accurate up to 0.0001 g/cm^3. The relative density difference $\Delta\rho/\rho_0=(\rho-\rho_0)/\rho_0$ with respect to the density of water ρ_0 is presented in Fig. 2 as a function of the concentration C at 20 °C. We recover the fact that the fluorescein mixture is denser than water and the alcohol mixture is lighter than water. It is also clear that the density difference depends linearly on the mass concentration of these dilutions, which allows one to fit the measurements by linear laws for the fluorescein,

$$\Delta\rho_{\mathrm{Fluo}}/\rho_0 = 0.447 C_{\mathrm{Fluo}}, \tag{1}$$

and for the alcohol,

$$\Delta\rho_{\mathrm{alcohol}}/\rho_0 = -0.169 C_{\mathrm{alcohol}}, \tag{2}$$

when the mass concentration is smaller than 0.01. These empirical laws are accurate to within 5% and are quite insensitive to the temperature because it is the difference with respect to the density of water which is given and not the absolute density. These formulas allow the creation of a mixture with the desired relative density difference down to 10^{-5}, even though it would be impossible to measure the density difference accurately below 10^{-3}. This is why these preliminary calibrations are extremely useful because it will be shown later that density differences on the order of 10^{-4} are sufficient to change the behavior of the flow dramatically. Moreover, by mixing the correct amount of fluorescein and alcohol (with densities of $+10^{-5}$ and -10^{-5}, respectively), it is possible to make a neutrally buoyant mixture that will be used as a test case.

The flow under consideration depends on three main dimensionless parameters. The aspect ratio H/R is kept constant at a value of 1.98. The Reynolds number $\mathrm{Re}=\Omega R^2/\nu$, ν being the kinematic viscosity of the water, is varied between 700 and 4000. The relative density difference $\Delta\rho/\rho_0$ between the mixture and the water is varied between -1×10^{-3} and 2×10^{-4}. There are three additional dimensionless parameters that are small in the experiments. As defined by Herrada and Shtern,[30] the Froude number $F=\Omega^2R/g$ (where $g=9.81$ ms^{-2} is the gravity) varies between 0.001 and 0.04. The Schmidt number $\mathrm{Sc}=\nu/\kappa$, κ being the molecular diffusivity in water, is on the order of 2000 for the fluorescein and on the order of 800 for ethanol. Finally, the volumic injection rate Q dimensionalized by $R^3\Omega$ varies between 8×10^{-5} and 0.02.

III. VORTEX BREAKDOWN VISUALIZATION WITH NEUTRALLY BUOYANT DYE MIXTURE

A test case has first been studied with neutrally buoyant dye by mixing alcohol and dye in order to have a density difference as small as possible. The flow is initiated and allowed to evolve for about 200 rotation periods before the dye injection in order to eliminate the transient effects. Then, the injection is started; the visualizations for various Reynolds numbers are shown in Fig. 3. For small Reynolds numbers [see Fig. 3(a)], the dye injected at the bottom is simply advected toward the top along the centerline. This is due to the recirculation which appears because the fluid is centrifugally pushed outward by the rotating top. It can be noted that the recirculation is opposite to that usually obtained in the literature[20,21,30] where rotating bottom lids are used instead of rotating top lid. When the Reynolds number is increased above a critical value of 1400, a bubble appears on the center axis of the cylinder as a consequence of the vortex breakdown. This bubble has an axial velocity opposite to the recirculation (i.e., toward the bottom), thus creating a stagnation point at the bottom of the bubble. This structure is very clear in Fig. 3(b) where a large bubble is surrounded at the

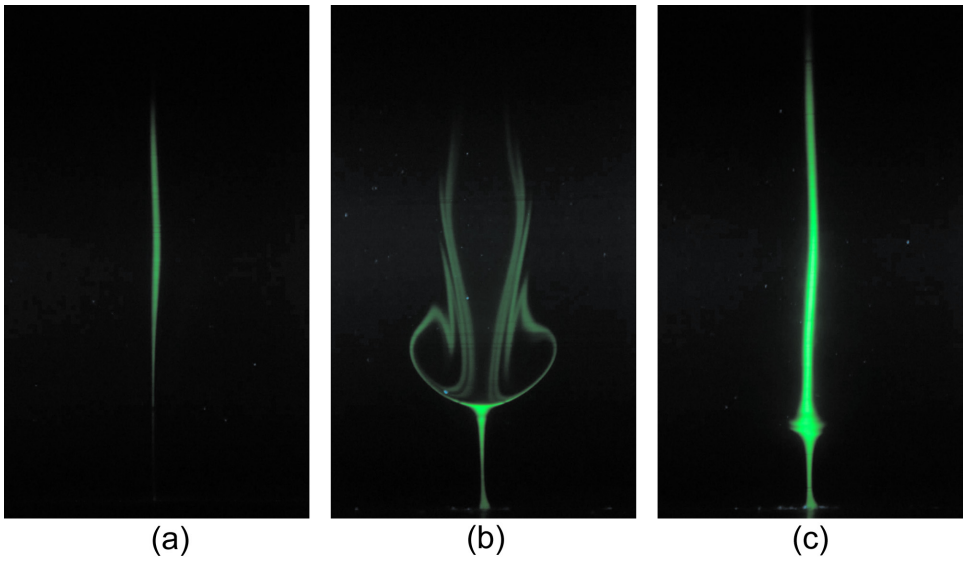

FIG. 3. (Color online) Dye visualization of vortex breakdown in the meridional plane with a neutrally buoyant dye ($\Delta\rho/\rho_0=0$) for a Reynolds number equal to (a) Re=1400, (b) Re=2060, and (c) Re=3030.

bottom by a saddle point and at the top by a smaller more elongated bubble. The presence of two bubbles is in excellent agreement with previous experimental results,[20] where two bubbles were observed above $H/R=1.95$ and even three bubbles around $H/R=3.35$. The size of the vortex breakdown bubble increases with the Reynolds number until Re$\sim$2000 and then decreases gradually up to Re=3000, where the bubble disappears completely. This is illustrated in Fig. 3(c) where the bubble has been replaced by a small undulation along the centerline, which is simply a consequence of small asymmetries in the experimental setup. These results are in excellent agreement with the literature where vortex breakdown has been observed for a Reynolds number between 1440 and 3000.

The temporal evolution of the dye after injection is shown on Fig. 4. The dye is first advected rapidly from the bottom to the stagnation point and slowly diverges radially [see Fig. 4(a)]. It is then advected around the bubble and exhibits large vertical undulations when it converges radially [see Fig. 4(b)]. These asymmetries are due to flow structural instability and experimental imperfections in the location of the injection hole and in the alignment of the rotating top disk.[38,40,41] At late stages, the dye slowly fills the two bubbles and becomes thicker due to the molecular diffusion [see Fig. 4(c)]. The structure observed in this experiment is similar to the structure found previously with a rotating bottom[20] except that it is upside down. This is because there

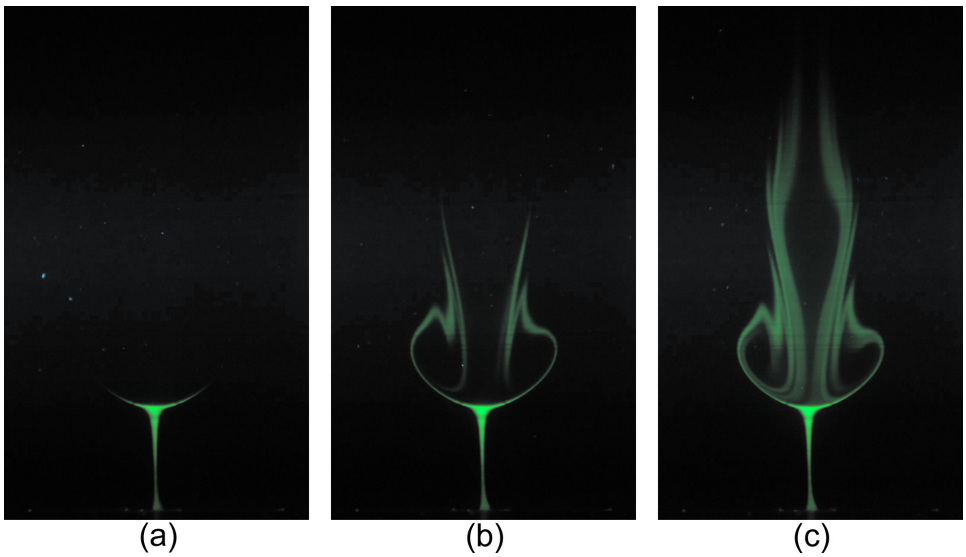

FIG. 4. (Color online) Temporal evolution of a neutrally buoyant dye ($\Delta\rho/\rho_0=0$) injected into the vortex breakdown at (a) $t\Omega=10$, (b) $t\Omega=60$, and (c) $t\Omega=140$ at Re=2060.

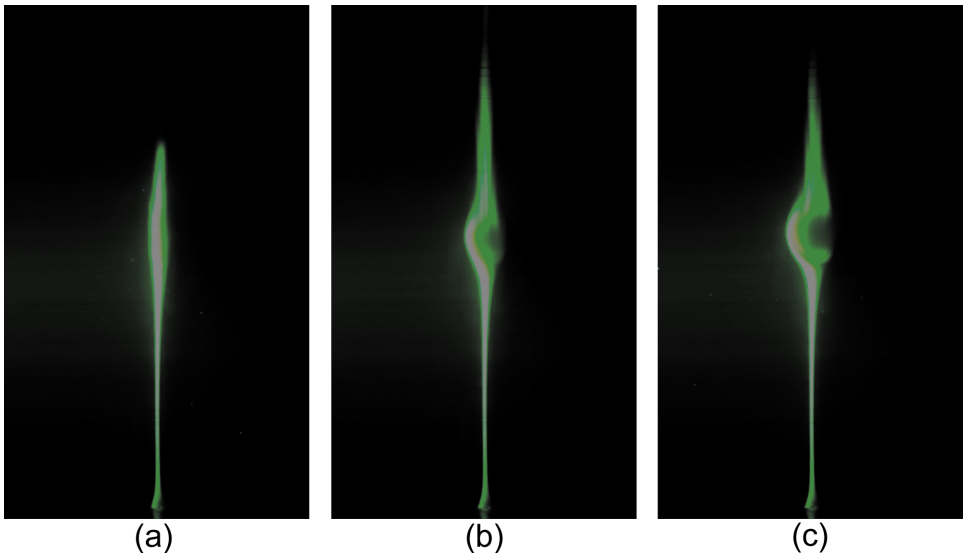

FIG. 5. (Color online) Temporal evolution of a dense dye ($\Delta\rho/\rho_0=0.75\times10^{-4}$) injected into the recirculating flow at a low Reynolds number (Re=1300). The images, taken approximately at (a) $t\Omega=100$, (b) $t\Omega=300$, and (c) $t\Omega=400$ show the clear formation of a bubble.

are no density effects. We are now going to study the case of a nonbuoyant dye mixture.

IV. DESTABILIZATION OF THE FLOW BY INJECTION OF DENSE DYE

Figure 5 shows an experiment for a Reynolds number (Re=1300) below the critical Reynolds number of vortex breakdown appearance ($Re_c=1400$). Before injection of the dye, the flow is stable without any vortex breakdown. Heavy dye is then injected and a pattern similar to Fig. 3(a) can be seen at early stages, as shown in Fig. 5(a): the dye flows upward along the centerline from the injection point. However, this behavior is only transient. After about 50 rotation periods, the dye accumulates and thickens, as shown in Fig. 5(b). After about 60 rotation periods, Fig. 5(c) shows the clear formation of a bubble at the center of the cylinder, characteristic of vortex breakdown. The destabilization of the flow can be easily understood because the heavy dye tends to sink due to gravity and thus counteracts the global recirculation and axial flow velocity, which enhances the bubble formation. It is striking to see that this destabilization occurs for a very small density difference: in this case $\Delta\rho/\rho_0$ is smaller than 10^{-4}. This may be understood because the sinking velocity of the dye needs to counteract the upward velocity at the center of the cylinder, which, close to the critical Reynolds number, is smaller than the global meridional recirculation, which is itself much smaller than the rotation induced by the disk. A very small density difference is thus sufficient to create a sinking velocity comparable to the upward recirculating velocity along the center axis of the cylinder.

The destabilization due to the heavy dye can be quantified by plotting the critical Reynolds number of vortex breakdown appearance as a function of the density difference $\Delta\rho/\rho_0$. This is plotted on the stability diagram of Fig. 6 where the vortex breakdown is present between the two solid lines. The unstable band of the Reynolds numbers increases rapidly when the density difference increases: the lower critical Reynolds number drops by a factor of 2 (from 1400 to 720) when the density difference increases up to 2×10^{-4}. This control by density effects is much more efficient than the use of a small rotating disk at the bottom which only modifies the critical Reynolds number by 15% when it rotates twice as fast as the top disk.[36] However, this control is limited to small density differences because the dye is not advected by the flow and simply spreads on the bottom of the cylinder if $\Delta\rho/\rho_0$ is larger than 2×10^{-4}. Finally, it should be noted that the bubble loses its steadiness if the dye is heavy enough (above a density difference of approximately 10^{-4}). The bubble was observed to lean off axis and then started to precess around the axis of the cylinder. This unsteadiness is very different from the axial periodic oscillation of the bubble that appears without dye injection at the high Reynolds numbers (larger than 2600 for this aspect ratio), as was found experimentally[20] and numerically.[42]

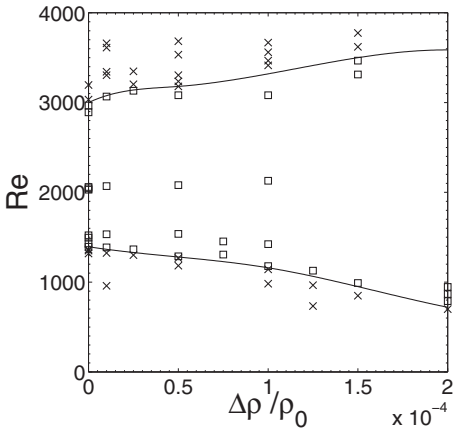

FIG. 6. Stability diagram of formation of vortex breakdown for a heavy dye. Experiments are represented by squares (□) to indicate the presence of a bubble and as crosses (×) when the flow is recirculating without a bubble. Solid lines are a fit of the experimental results.

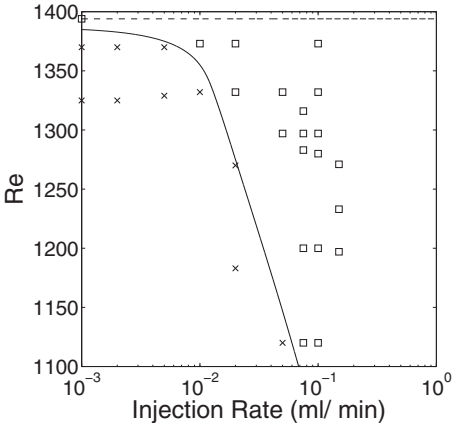

FIG. 7. Stability diagram of formation of the vortex breakdown as a function of the volumic injection rate Q for a fixed density difference $\Delta\rho/\rho_0=0.5\times10^{-4}$. Squares (□) represent experiments with vortex breakdown and crosses (×) without vortex breakdown. The solid line is a fit to the experimental data. The dashed line corresponds to the critical Reynolds number for a neutrally buoyant dye.

As noted by Herrada and Shtern,[30] there is another effect due to the density difference $\Delta\rho/\rho_0$. Since the flow is rotating close to the top spinning disk, there is a centrifugal acceleration $\mathbf{a_c}$ which creates a centrifugal force on the heavy dye. The dye tends to flow radially outward at the top of the cylinder, which enhances the global recirculation and thus reduces the formation of the vortex breakdown. This effect has been observed in the numerical simulations of Herrada and Shtern[30] in the absence of gravity, but it seems to be negligible in our experiments. In fact, it can be inferred from their results that the effect of the centrifugal convection counteracts the effect of the gravitational convection when the Froude number F (which is the ratio between the centrifugal force ΩR^2 and the gravity g) is roughly equal to 100. In our experiments, the Froude number is on the order of 0.01 and the effect of the gravitational convection is thus 10 000 times larger than the effect of the centrifugal convection. This is why our results can be explained by the effect of the gravity alone.

Finally, we measure the sensitivity of the flow with respect to the injection rate. Figure 7 shows the stability diagram of the vortex breakdown as a function of the injection rate for a fixed density difference $\Delta\rho/\rho_0=0.5\times10^{-4}$. At small injection rates, the critical Reynolds number is almost constant until $Q=0.01$ ml/min, where it starts to decrease rapidly. This means that when the injection rate increases, the flow becomes more sensitive to the density difference $\Delta\rho/\rho_0$. It might thus be possible to decrease by more than a factor of 2 the critical Reynolds number of appearance of the vortex breakdown. This once again emphasizes the strong effect of the density difference on the destabilization of the flow.

V. A NEW VORTEX BREAKDOWN STRUCTURE FOR LIGHT DYE

We now present the effect of a dye which is lighter than the surrounding fluid. The temporal evolution of the flow after injection of a light dye ($\Delta\rho/\rho_0=-2.3\times10^{-4}$) is presented in Fig. 8(a). The Reynolds number is chosen above the critical Reynolds number ($\mathrm{Re}_c=1400$) such that the flow contains a strong vortex breakdown bubble before the injection of dye. When the dye is injected, it is advected rapidly by the flow up to the stagnation point, as shown in Fig. 8(a). While the mixture accumulates at the stagnation point, some dye flows around the bubble. The accumulation of the dye increases its buoyancy force and thus allows the dye to pierce through the bubble, as shown in Fig. 8(b). At late stages, the dye creates a thin jet along the centerline, which goes through the whole bubble up to the top disk [Fig. 8(b)]. It is striking to see that this jet does not disrupt the vortex breakdown, which is still present as a leaf shape, although the visualization is not as clear because less dye is advected

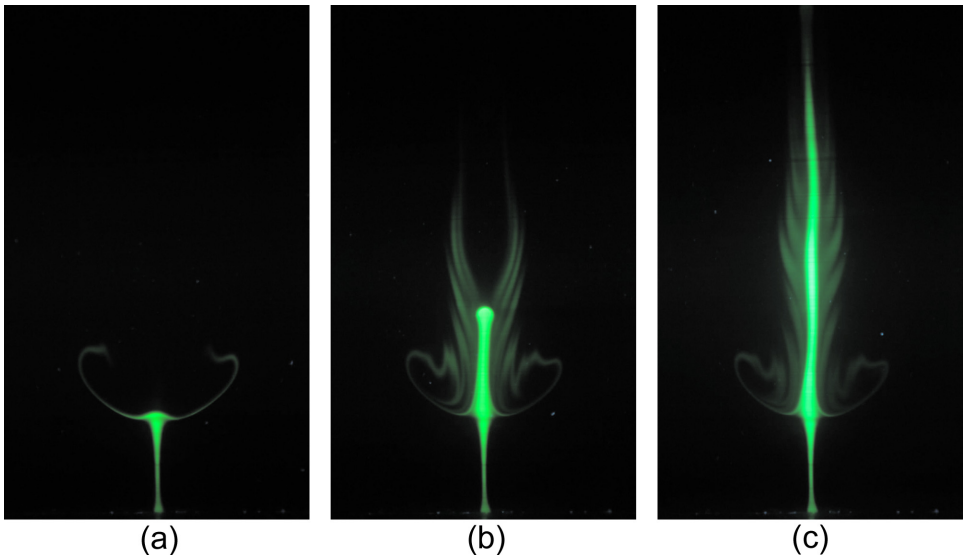

FIG. 8. (Color online) Temporal evolution of a light dye $\Delta\rho/\rho_0=-2.267\times10^{-4}$ injected in a vortex breakdown at Re=2423. The pictures are taken approximately at (a) $t\Omega=25$, at (b) $t\Omega=60$, and at (c) $t\Omega=110$.

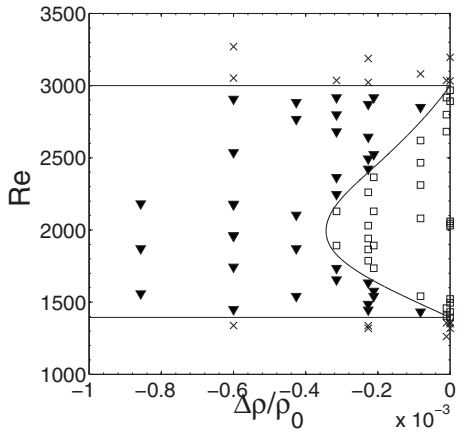

FIG. 9. Stability diagram of formation of vortex breakdown for a light dye. Experiments are represented by squares (□) to indicate the presence of a bubble and as crosses (×) when the flow is recirculating without a bubble. Solid lines are a fit of the experimental results. A new regime represented by solid triangles depicts the formation of vortex breakdown with a jet piercing through the bubble as shown in Fig. 8.

around the bubble. It can be noted that this evolution is very rapid: it happens after approximately ten rotation periods, whereas the destabilization of the flow by the dense dye happened in 50 rotation periods.

This new structure of the vortex breakdown is plotted in the stability diagram of Fig. 9 as solid triangles. It is observed for all Reynolds numbers when the dye is light enough ($\Delta\rho/\rho_0 < -3\times10^{-4}$). When the dye is not light enough, the mixture accumulates at the stagnation point but does not gain enough buoyancy force. It is thus advected around the bubble and leads to the well-known structure of the vortex breakdown found in Fig. 4. This classical regime is indicated by squares on the stability diagram. It is surprising to see that the light jet is not able to destroy the vortex breakdown bubble: the transition between the stable flow and the vortex breakdown with a buoyant jet is independent of the density difference. To conclude, even if the presence of a light dye is not able to destroy the vortex breakdown, a small variation of the dye density is able to create a radical change of the structure of the flow.

The sensitivity of the flow with respect to the dye density poses a major question concerning the results of the literature.[5,39] Indeed, most of the experimental results have been obtained by dye visualizations, where the dye was probably heavier than the working fluid. However, since these experiments have been done with a rotating bottom instead of a rotating top, the density effects are reversed: the heavy dye enhances the recirculation and thus tends to prevent the vortex breakdown. As was mentioned in this section, the breakdown bubble cannot be destroyed by the dye and this is why the results of the literature (for a rotating bottom) are not influenced by the injection of a dense dye.

VI. VORTEX RING INTERACTION WITH VORTEX BREAKDOWN

We wish to study the interaction of a vortex ring generated at the bottom with the vortex breakdown. It is similar to an injection of light dye because the vortex ring contains some momentum and pushes the fluid toward the top. In these experiments, a Reynolds number of 2000 is selected such that a strong breakdown bubble is formed in the cylinder. Additionally, a neutrally buoyant dye is used to ensure that the visualization process does not modify the flow. Before the vortex ring is created, a small amount of fluorescein mixture is injected to visualize the breakdown bubble. The vortex ring is then created by mechanically pinching the tube connected to the injection hole.

In the first experiment, a strong vortex ring is produced and its interaction is visualized in Fig. 10. The vortex ring rapidly reaches the stagnation point and penetrates through the breakdown bubble. As the vortex ring travels through the breakdown region, the ring decelerates and its diameter in-

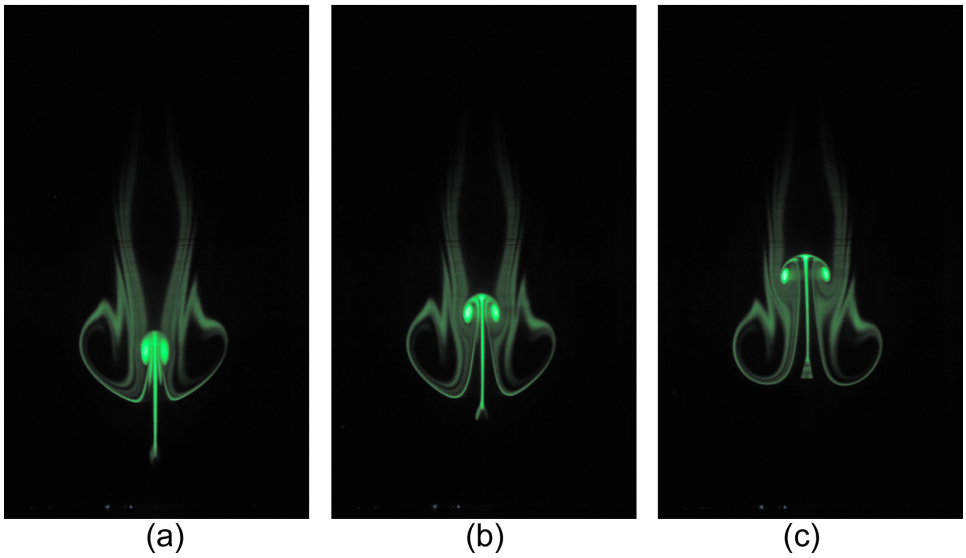

FIG. 10. (Color online) Temporal evolution of a strong vortex ring impacting the vortex breakdown at Re=2000, visualized with a neutrally buoyant dye ($\Delta\rho/\rho_0=0$).

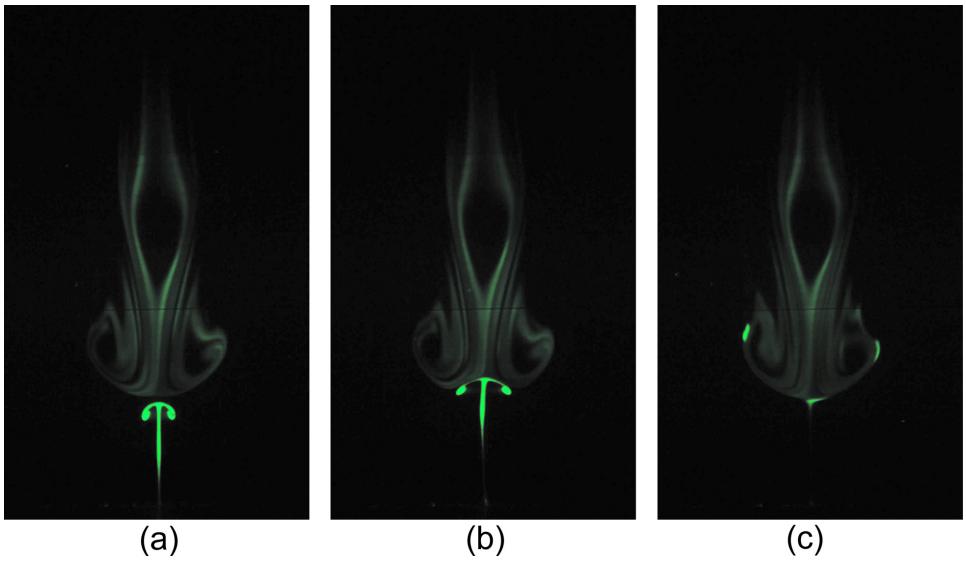

FIG. 11. (Color online) Temporal evolution of a weak vortex ring impacting the vortex breakdown at Re=2000, visualized with a neutrally buoyant dye ($\Delta\rho/\rho_0=0$).

creases. The breakdown bubble is very weakly modified by the presence of the vortex ring. This shows once again the robustness vortex breakdown to disturbances. This behavior is very similar to the one shown in Fig. 8, where the light jet pierces through the bubble. Although the characteristics of the vortex ring were not measured accurately by particle image velocimetry (PIV) measurements, they were estimated using the position and the size of the ring on the dye visualizations. The vertical velocity of the vortex ring decreases rapidly due to viscous effects and due to the interaction with the vortex breakdown but it was approximately equal to 4.4 cm/s (or 0.7 in dimensionless units) before reaching the stagnation point (i.e., for $z/H \approx 0.15$). The diameter of the ring increases slowly and is on the order of 2.5 mm (i.e., $0.07R$) before the impact with the vortex breakdown.

A second experiment is conducted for a weak vortex ring interacting with the vortex breakdown, as visualized in Fig. 11. The vortex ring travels upward along the centerline and decelerates at the stagnation point. Instead of penetrating through the breakdown bubble, the ring widens and is advected around the breakdown. The strength of the vortex ring decreases very fast, leading to a simple blob of scalar without any vorticity at late stages. The velocity of the vortex ring was estimated to be equal to 2.2 cm/s (or 0.35 in dimensionless units) and its diameter is equal to 2.5 mm (or $0.07R$) before the impact with the vortex breakdown (i.e., for $z/H \approx 0.15$).

These two experiments show that the behavior of a vortex ring impacting a vortex breakdown is similar to a jet of light dye. If the vortex ring is strong enough (or if the dye is light enough), the vortex ring (or the dye) will pierce through the bubble. If the vortex ring is too weak (or if the dye is not light enough), the vortex ring (or the dye) will be advected around the bubble. However, in no cases investigated could the vortex ring (or the light jet) destroy the vortex breakdown bubble.

VII. CONCLUSIONS

We have shown that the density of the dye used for visualizations has a significant effect on the vortex breakdown structure and stability. This effect has been observed and measured experimentally in a cylinder with a rotating top lid when the dye is injected at the bottom. On one hand, a denser dye is able to induce vortex breakdown and thus widens the range of critical Reynolds numbers for which the bubble appears. This can be explained by the sinking velocity of the dye which counteracts the global recirculation and thus favors the formation of a stagnation point and creation of the bubble. This dramatic effect can reduce the critical Reynolds number by a factor of 2 for the extremely small density difference of 0.02% at a very small injection rate. On the other hand, a light dye does not destroy the vortex breakdown but leads to a new structure where the jet of dye pierces through the breakdown bubbles. This new structure appears above a critical density difference on the order of 0.03%, which is also extremely small. Finally, we have shown that a vortex ring impacting the vortex breakdown has the same behavior as a light jet: it can either penetrate through the bubble or be advected around it depending on the momentum of the vortex ring.

These results indicate that a very small density difference can be used to control the vortex breakdown in a very efficient way. This effect might have great implications in geophysical flows where the presence of water vapor at the bottom of the tornadoes (e.g., tornadic waterspouts) might have a large effect on the structure of the tornadoes. Unfortunately, it might not be very suited to aeronautical or combustion applications since it occurs only for a vortex with a vertical axis. In bioengineering, this effect can be important for bioreactors since the injection of a dense or light nutrient might have a large effect on the structure of the flow inside the bioreactor. Moreover, the new structure of a light jet

penetrating through the vortex breakdown could be used to feed the cells located in the bubble without having to put a probe close to the cells. This is of great interest for suspension cells which need to grow far from any boundary. Finally, the sensitivity of the flow to the density difference could be used to control the shear stress experienced by the cells, which is known to induce differentiation for stem cells.

[1]S. Leibovich, "The structure of vortex breakdown," Annu. Rev. Fluid Mech. **10**, 221 (1978).
[2]D. L. Kohlman and W. H. Wentz, "Vortex breakdown on slender sharp-edged wings," J. Aircr. **8**, 156 (1971).
[3]M. G. Hall, "Vortex breakdown," Annu. Rev. Fluid Mech. **4**, 195 (1972).
[4]M. V. Lowson and A. J. Riley, "Vortex breakdown control by delta wing geometry," J. Aircr. **32**, 832 (1995).
[5]M. P. Escudier, "Vortex breakdown: Observations and explanations," Prog. Aerosp. Sci. **25**, 189 (1988).
[6]O. R. Burggraf and M. R. Foster, "Continuation or breakdown in tornado like vortices," J. Fluid Mech. **80**, 685 (1977).
[7]R. P. Davies-Jones, "Tornado dynamics," in *Thunderstorms: A Social, Scientific, and Technological Documentary*, edited by E. Kessler (University of Oklahoma Press, Nolan, 1983), Vol. 2, p. 297.
[8]A. K. Gupta, D. G. Lilley, and N. Syred, *Swirl Flows* (Abacus, Kent, England, 1984).
[9]J. Dusting, J. Sheridan, and K. Hourigan, "A fluid dynamics approach to bioreactor design for cell and tissue culture," Biotechnol. Bioeng. **94**, 1196 (2006).
[10]G. A. Thouas, J. Sheridan, and K. Hourigan, "A bioreactor model of mouse tumor progression," J. Biomed. Biotechnol. **9**, 327 (2007).
[11]J. K. Harvey, "Some observations of the vortex breakdown phenomenon," J. Fluid Mech. **14**, 585 (1962).
[12]T. Sarpkaya, "On stationary and travelling vortex breakdowns," J. Fluid Mech. **45**, 545 (1971).
[13]J. H. Faler and S. Leibovich, "An experimental map of the internal structure of a vortex breakdown," J. Fluid Mech. **86**, 313 (1978).
[14]H. Ludwieg, "Zur erklarung der instabilitat der uber angestellten delta-flugeln auftretenden freien wirbelkerne," Z. Flugwiss. **10**, 242 (1962).
[15]T. B. Benjamin, "Theory of the vortex breakdown phenomenon," J. Fluid Mech. **14**, 593 (1962).
[16]H. B. Squire, "Analysis of the vortex breakdown phenomenon. Part 1," Department of Aeronautics, Imperial College Report No. 102, 1962.
[17]S. Wang and Z. Rusak, "The dynamics of a swirling flow in a pipe and transition to axisymmetric vortex breakdown," J. Fluid Mech. **340**, 177 (1997).
[18]H. U. Vogel, "Experimentelle ergebnisse über die laminare strömung in einem zylindrischen gehaüse mit darin rotierender scheibe," Max-Planck-Institut für Strömungsforschung Technical Report Bericht 6, 1968.
[19]B. Ronnenberg, "Ein selbstjustierendes 3-komponenten-LDA nach dem vergleighstrahlverfaren, angewendt für untersuchungen in einer stationären zylindersymmetrischen drehströmung mit einem rühckströmgebiet," Max-Planck-Institut für Strömungsforschung Technical Report Bericht 20, 1977.
[20]M. P. Escudier, "Observations of the flow produced in a cylindrical container by a rotating endwall," Exp. Fluids **2**, 189 (1984).
[21]A. Spohn, M. Mory, and E. J. Hopfinger, "Observations of vortex breakdown in an open cylindrical container with rotating bottom," Exp. Fluids **13**, 70 (1993).
[22]H. J. Lugt and M. Abboud, "Axisymmetric vortex breakdown in a container with a rotating lid," J. Fluid Mech. **179**, 179 (1987).
[23]G. P. Neitzel, "Streak-line motion during steady and unsteady axisymmetric vortex breakdown," Phys. Fluids **31**, 958 (1988).
[24]J. M. Lopez, "Axisymmetric vortex breakdown. Part 1: Confined swirling flow," J. Fluid Mech. **221**, 533 (1990).
[25]G. L. Brown and J. M. Lopez, "Axisymmetric vortex breakdown. Part 2: Physical mechanism," J. Fluid Mech. **221**, 553 (1990).
[26]J. M. Lopez and A. D. Perry, "Axisymmetric vortex breakdown. Part 3: Onset of periodic flow and chaotic advection," J. Fluid Mech. **234**, 449 (1992).
[27]S. Bhattacharyya and A. Pal, "Axisymmetric vortex breakdown in a filled cylinder," Int. J. Eng. Sci. **36**, 555 (1998).
[28]D. T. Valentine and C. C. Jahnke, "Flow induced in a cylinder with both ends walls rotating," Phys. Fluids **6**, 2702 (1994).
[29]F. Gallaire, J. M. Chomaz, and P. Huerre, "Closed-loop control of vortex breakdown: A model study," J. Fluid Mech. **511**, 67 (2004).
[30]M. A. Herrada and V. Shtern, "Control of vortex breakdown by temperature gradients," Phys. Fluids **15**, 3468 (2003).
[31]D. Lo Jacono, J. N. Sørensen, M. C. Thompson, and K. Hourigan, "Control of vortex breakdown in a closed cylinder with a small rotating rod," J. Fluids Struct. **24**, 1278 (2008).
[32]B. Jørgensen, J. Sørensen, and N. Aubry, "Control of vortex breakdown in a closed cylinder with a rotating lid," Theor. Comput. Fluid Dyn. **24**, 483 (2010).
[33]B. T. Tan, K. Y. S. Liow, L. Mununga, M. C. Thompson, and K. Hourigan, "Simulation of the control of vortex breakdown in a closed cylinder using a small rotating disk," Phys. Fluids **21**, 024104 (2009).
[34]P. Yu, T. S. Lee, Y. Zeng, and H. T. Low, "Effects of conical lids on vortex breakdown in an enclosed cylindrical chamber," Phys. Fluids **18**, 117101 (2006).
[35]H. Husain, V. Shtern, and F. Husain, "Control of vortex breakdown by addition of near-axis swirl," Phys. Fluids **15**, 271 (2003).
[36]L. Mununga, K. Hourigan, and M. C. Thompson, "Confined flow vortex breakdown control using a small rotating disk," Phys. Fluids **16**, 4750 (2004).
[37]S. Khalil, K. Hourigan, and M. C. Thompson, "Effects of axial pulsing on unconfined vortex breakdown," Phys. Fluids **18**, 038102 (2006).
[38]M. C. Thompson and K. Hourigan, "The sensitivity of steady vortex breakdown bubbles in confined cylinder flows to rotating lid misalignment," J. Fluid Mech. **496**, 129 (2003).
[39]A. Spohn, M. Mory, and E. J. Hopfinger, "Experiments on vortex breakdown in a confined flow generated by a rotating disc," J. Fluid Mech. **370**, 73 (1998).
[40]M. Brøns, W. Z. Shen, J. N. Sørensen, and W. J. Zhu, "The influence of imperfections on the flow structure of steady vortex breakdown bubbles," J. Fluid Mech. **578**, 453 (2007).
[41]M. Brøns, M. Thompson, and K. Hourigan, "Dye visualization near a three-dimensional stagnation point: Application to the vortex breakdown bubble," J. Fluid Mech. **622**, 177 (2009).
[42]A. Y. Gelfat, P. Z. Bar-Yoseph, and A. Solan, "Three-dimensional instability of axisymmetric flow in a rotating lid-cylinder enclosure," J. Fluid Mech. **438**, 363 (2001).